



Darkwa, Jo and Su, O. and Zhou, T. (2015) Evaluation of thermal energy dynamics in a compacted high-conductivity phase-change material. *Journal of Thermophysics and Heat Transfer*, 29 (2). pp. 291-296. ISSN 1533-6808

**Access from the University of Nottingham repository:**

<http://eprints.nottingham.ac.uk/47493/1/NPap.THT.pdf>

**Copyright and reuse:**

The Nottingham ePrints service makes this work by researchers of the University of Nottingham available open access under the following conditions.

This article is made available under the University of Nottingham End User licence and may be reused according to the conditions of the licence. For more details see: [http://eprints.nottingham.ac.uk/end\\_user\\_agreement.pdf](http://eprints.nottingham.ac.uk/end_user_agreement.pdf)

**A note on versions:**

The version presented here may differ from the published version or from the version of record. If you wish to cite this item you are advised to consult the publisher's version. Please see the repository url above for details on accessing the published version and note that access may require a subscription.

For more information, please contact [eprints@nottingham.ac.uk](mailto:eprints@nottingham.ac.uk)

# **Evaluation of thermal energy dynamics in a compacted high conductivity phase change material**

**J. Darkwa\*, O. Su, T. Zhou**

Centre for Sustainable Energy Technologies,  
University of Nottingham, Ningbo, China, 315100  
Tel: +86 574 88180255; Fax: +86 574 88180313

## **ABSTRACT**

This study evaluates the concept of developing a non-deform phase change energy storage material possessing higher thermal conductivity and energy storage density through pressure compaction process. The theoretical and experimental investigations have shown that the technique is able to reduce porosity and increase conductivity and energy storage density of a composite material. Even though there was some measure of plastoelasticity due to decompression, the average porosity was reduced from 62% to 23.8% at a relatively low compaction pressure of 2.8MPa without any structural damage to the tested sample. The mean energy storage density increased by 97% and the effective thermal conductivity also increased by twenty five times despite 10% reduction in its latent heat capacity. There is however the need for further development towards minimising the effect of decompression and achieving stronger energy storage tablets at relatively low compaction force.

**Key words:** phase change material; non-deformed; tablet; energy storage density

*\*E-mail of corresponding author: jo.darkwa@nottingham.ac.uk*

## Nomenclature

		<i>Greek letters</i>	
$C$	a constant	$\varepsilon$	porosity
$C_p$	specific heat (J/kg·K)	$\rho$	density (kg/m <sup>3</sup> )
$d$	diameter of the sample (m)	$\tau$	time (s)
$E$	specific energy storage capacity (J/m <sup>3</sup> )	$\varphi$	volume fraction
$H$	specific latent enthalpy (J/kg)		
$h$	thickness of tablets (m)	<i>Subscripts</i>	
$k$	thermal conductivity (W/m·K)	$a$	air
$m$	mass weight (kg)	$b$	bulk
$P$	pressure (Pa)	$e$	effective
$T$	temperature (K)	$l$	latent heat
$V$	volume (m <sup>3</sup> )	$P$	PCM
$X$	Reciprocal of yield pressure (1/ Pa)	$R$	relative
		$s$	sensible heat
		$y$	yield

## 1. 0: INTRODUCTION

Current statistics on energy usage show that the building sector consumes approximately 40% of the world's electricity supply for various types of building services systems[1]. It is also estimated that 85% of a building's gas emissions is caused by heating, cooling and lighting activities and that commercial buildings produce approximately a third of energy-related carbon emissions worldwide [2]. In its Energy Efficiency in Buildings Action 2010 report (EEB in Action 2010) the World Business Council for Sustainable Development (WBCSD) outlined how energy use in buildings can be cut by 60% by 2050 through a combination of public policies, technological innovation, informed customer choices, and smart business decisions [3].

Application of phase change materials (PCMs) in buildings is considered as an effective innovative technology for reducing energy consumption. For example an experimental composite PCM concrete floor tested by Entrop *et al.* [4] achieved 16% reduction and 7% increase in the mean summer and winter floor temperatures respectively. Theoretical investigation by Darkwa and O'Callaghan [5] showed that a laminated PCM wall board with a narrow phase-change zone was capable of increasing winter minimum room temperature by about 17% more than a randomly mixed type. Darkwa [6] further investigated the laminated PCM concept in a buried concrete pipe and reported significant cooling capacity enhancement but with a turbulent generated type of air flow. Hunger *et al.* [7] studied the impact of PCM in self-compacting concrete material and achieved significant improvement in the thermal performance of concrete but observed significant loss in strength. Ceron *et al.* [8] reported 15% energy performance enhancement in a floor tile containing paraffin based PCM.

However, PCMs have so far achieved limited applications in buildings due to their relatively poor thermal response and other integration barriers. To this end, some research efforts towards enhancement have been carried out by various investigators. Sarl [9] developed and tested an experimental composite PCM with high density polyethylene (HDPE) and obtained an increase of 24% in its thermal conductivity. Li *et al* [10] investigated a novel form-stable phase change material comprising of micro-encapsulated paraffin and HDPE material and also achieved up to 25% thermal enhancement. Other researchers such as Borreguero *et al.* [11], Feldman *et al.* [12] and Darkwa and Zhou [13] have further evaluated different composite PCM materials and achieved good heat transfer enhancements but did report reductions in energy storage densities. In this current study it is proposed to overcome these barriers through pressure compaction technique whereby an atomized metal powder of predetermined size is combined with PCM particles in a pressure controlled environment to obtain an enhanced composite material.

## **2.0: THEORETICAL CONCEPT**

The concept is based on compacting micro-encapsulated phase change material (MEPCM) and a high conductivity material in a powder form to obtain composite phase change material tablets. The concept is intended to reduce porosity and thereby increase energy storage density and thermal conductivity in the composite tablets. The process involves the simultaneous compression and consolidation of a two-phase (particulate solid-gas) system due to an applied force. The principles of compaction and decompression in powder tableting have been widely studied and reviewed in various sources [14-15] and therefore would not be covered in this study. However,

the key governing principles and theories relevant to this study shall be highlighted in the following sections.

## 2.1 Compaction and decompression processes

According to Marshal [16] and Bodga [17] powder compaction processes do normally result in particle rearrangement, elastic and plastic deformation as well as particle fragmentation. The relationship between porosity and compaction pressure could therefore be expressed mathematically by Heckel's equation [18] being the most popular method for determining the volume reduction mechanism under applied force. The method is based on the assumption that powder compression follows first order kinetics with the interparticulate pores as the reactants and the densification of the powder as the product (see Eq. 1). The equation indicates that the degree of compact densification with increasing compression pressure is directly proportional to the porosity as follows:

$$\frac{d\rho_R}{dP} = X\varepsilon \quad (1)$$

Where

$\rho_R$  is the relative density at pressure, P

$\varepsilon$  is the fractional void or porosity of the material.

The porosity can also be expressed as:

$$\varepsilon(\tau) = 1 - \rho_{R(\tau)} = 1 - \frac{V_P}{V(\tau)} \quad (2)$$

Where  $V_\tau$  and  $V_p$  are the volume at any applied load and the volume at theoretical zero porosity respectively.

Therefore Eq. 1 can be re-written as:

$$\frac{d\rho_R}{dP} = X(1 - \rho_{R(\tau)}) \quad (3)$$

It can further be expressed as:

$$\ln[1/(1 - \rho_{R(\tau)})] = XP(\tau) + C$$

$$\ln\left(\frac{1}{\varepsilon}\right) = XP(\tau) + C = \frac{P(\tau)}{P_y} + C \quad (4)$$

By plotting the value of  $\ln [1/(\varepsilon)]$  against applied pressure,  $P(\tau)$ , yields a linear graph having slope,  $X$  and intercept,  $C$ . Where inverse of  $X$  is the yield pressure,  $P_y$  of the material. It also relates inversely to the ability of the material to deform plastically under pressure.

Decompression stage normally follows compression process as the applied load is removed. This phenomenon was expressed by David and Augsburger [19] that the same deformation characteristics that are experienced during compression play a role during decompression process. They further explained that materials which undergo more plastic flow often form strong tablets at relatively low compaction force.

## 2.2 Thermophysical properties

Since the process is intended to increase the effective thermal conductivity and energy storage density of a composite phase change material, the relevant thermophysical properties shall be examined as follows.

### 2.2.1 Effective thermal conductivity ( $k_e$ )

According to Kohout *et al.* [20], there are two basic arrangements i.e. the series and parallel models that can be used to analyse the upper and lower bands of effective thermal conductivities ( $k_e$ ) in composite materials.

*Series model*

$$k_e^{-1} = \sum \varphi_i^{-1} k_i \quad (5)$$

*Parallel model*

$$k_e = \sum \varphi_i k_i \quad (6)$$

Where

$k_i$  is the thermal conductivity of material  $i$

$\varphi_i$  is the volume fraction of material  $i$

However for a porous composite material consisting of MEPCM and a heat conducting material say aluminium powder ( $Al_p$ ), the volume fraction can be expressed as:

$$\varphi_P + \varphi_{Al} + \varepsilon = 1 \quad (7)$$

The effective conductivity of the series and parallel models can also be expressed as:

*Series model*

$$\frac{1}{k_e} = \frac{\varphi_{Al}}{k_{Al}} + \frac{\varphi_P}{k_P} + \frac{\varepsilon}{k_a} = \frac{1-\varepsilon-\varphi_P}{k_{Al}} + \frac{\varphi_P}{k_P} + \frac{\varepsilon}{k_a} = \frac{1-\varepsilon}{k_{P'}} + \frac{\varepsilon}{k_a} = \frac{k_a \cdot (1-\varepsilon) + k_{P'} \cdot \varepsilon}{k_{P'} \cdot k_a} \quad (8)$$

Eq. 8 could also be expressed in dimensionless form as:

$$\frac{k_e}{k_{P'}} = \frac{k_a}{(k_{P'} - k_a) \cdot \varepsilon + k_a} \quad (9)$$

Where;

$$\frac{1}{k_{P'}} = \frac{(1-\varepsilon-\varphi_P) \cdot k_P + \varphi_P \cdot k_{Al}}{(1-\varepsilon) \cdot k_{Al} \cdot k_P}$$

$k_a$ ,  $k_{Al}$  and  $k_P$  are the thermal conductivities of air void, aluminium powder and MEPCM respectively ( $k_{Al} > k_P > k_a$ )

$\varepsilon$  is the porosity fraction of the composite material ( $0 \leq \varepsilon \leq 1$ )

*Parallel model*

$$k_e = \varphi_{Al} \cdot k_{Al} + \varphi_P \cdot k_P + \varepsilon \cdot k_a \quad (10)$$

By substituting the value of  $\varphi_{Al}$  Eq. 10 can be rewritten as:



$$k_e = (k_a - k_p'') \cdot \varepsilon + k_p'' \quad (11)$$

$$\text{Where } k_p'' = \frac{(1-\varepsilon-\varphi_P) \cdot k_{Al} + \varphi_P \cdot k_P}{(1-\varepsilon)}$$

It could also be restructured in a dimensionless form as:

$$\frac{k_e}{k_p''} = \left( \frac{k_a}{k_p''} - 1 \right) \cdot \varepsilon + 1 \quad (12)$$

Now by considering Eqs. 9 and 12, the relationship between conductivity and the composite material porosity can be represented graphically in Fig. 1. It shows that the minimum and maximum bands for  $k_e$  do occur in the series and the parallel models respectively. It is also clear that lower porosity levels promote higher effective conductivities.

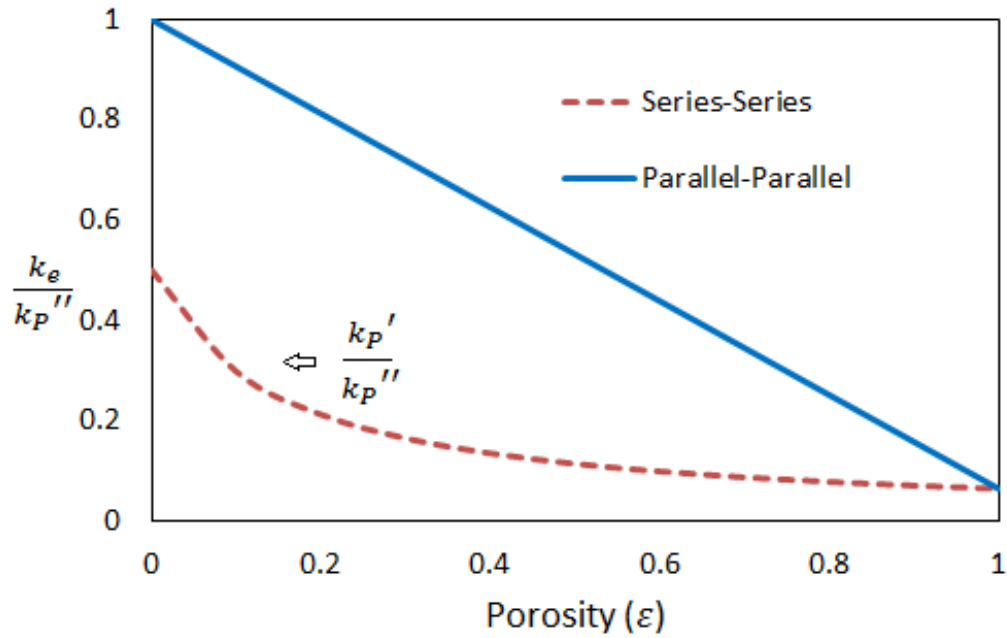


**Figure 1:** Porosity versus effective thermal conductivity

### 2.3 Energy storage density (E)

The total energy storage in the composite material may be computed as the sum of the sensible and latent heat per unit volume:

$$E = E_s + E_l = \rho \cdot \int_{T_0}^{T_1} C_p dT + \rho \cdot H \quad (13)$$

Where:

$$\rho = \rho_p \cdot (1 - \varepsilon) \quad (14)$$

Therefore;

$$E = \rho_p \cdot (1 - \varepsilon) \cdot \left( H + \int_{T_0}^{T_1} C_p dT \right) = E_p \cdot (1 - \varepsilon) \quad (15)$$

By using Eq. 15, the relationship between energy storage density and porosity can be explained in Fig. 2. Analysis of the graph clearly indicates that lower porosity ratio promotes higher energy storage density.

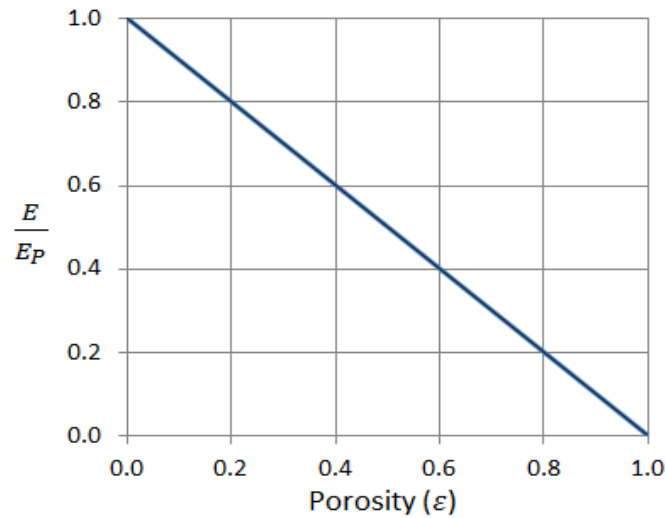


**Figure 2:** Energy storage density versus porosity

### 3.0 MATERIAL CHARACTERIZATION

Commercially available micro-encapsulated phase change material (heptadecane) and aluminium powder as a heat enhancement material were selected as the base materials for the composite material. However, the following initial tests were conducted on the materials to confirm their thermophysical properties.

#### 3.1 Particle size analysis

According to various publications such as Fichtner *et al.* [21] the size and characteristics of particles do affect the stability, chemical reactivity, opacity, viscosity, porosity and mechanical strength of tablets. In this regard particle size analyser equipment, (Bettersize type 2000) was used to establish the true sizes of the phase change material and the aluminium powder. The results are presented in Figs. 3 and 4.

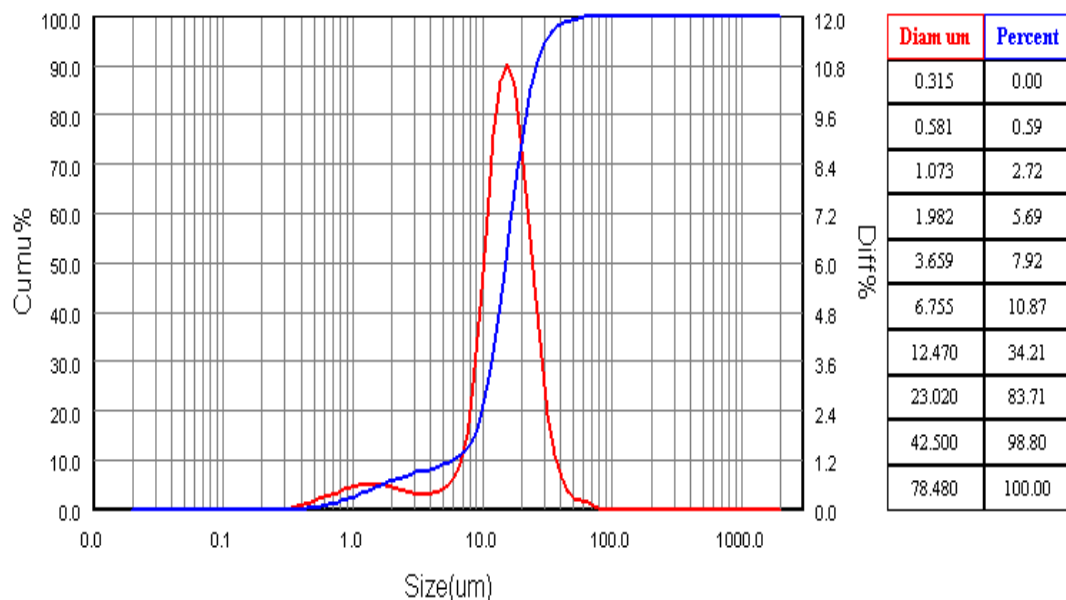


**Figure 3:** Particle sizing of MEPCM sample

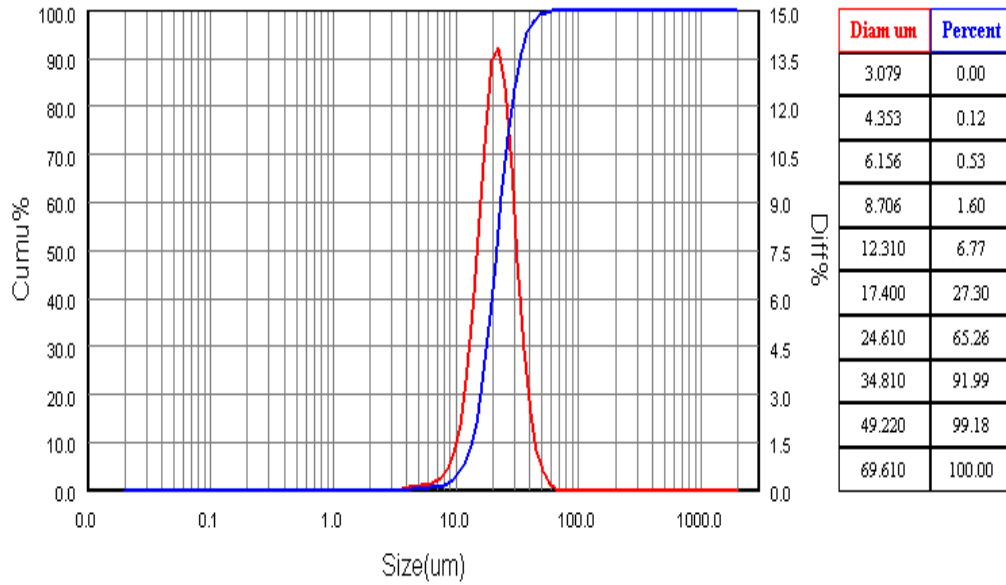


**Figure 4:** Particle sizing of Aluminium (Al) powder

### 3.2 Determination of total porosity

Total porosity of a material may be defined as that fraction of the bulk material volume that is not occupied by solid matter. In this classification, the well-known Archimedes' method was used and applied in Eq. 16 to determine the material porosity. The MEPCM sample was initially weighed dry and then weighed again when it was made fully saturated with water. The difference in weight between the dry and saturated samples was then noted and with the density of water known, the pore volume ( $V_a$ ) was determined. The bulk volume ( $V_b$ ) was also determined using the same Archimedes' method.

$$\varepsilon = \frac{V_a}{V_b} = \frac{V_b - V_P}{V_b} \quad (16)$$

### 3.3 Latent heat capacity

Differential scanning calorimetric (DSC6220 SII Nanotechnology) equipment was used in determining the enthalpies of fusion and melting temperature of the MEPCM sample in accordance with ISO 11357 Standards under the dynamic testing method.

In order to establish repeatability of the data the sample was tested 5 times under atmospheric air pressure and at a heating rate of 2°C/min from 5°C to 50°C as shown in Fig. 5. The summarised results in Tab. 1, give an average latent heat value of 124.8kJ/kg and a melting temperature of 22.2°C thus confirming the sample as an encapsulated n-heptadecane material.

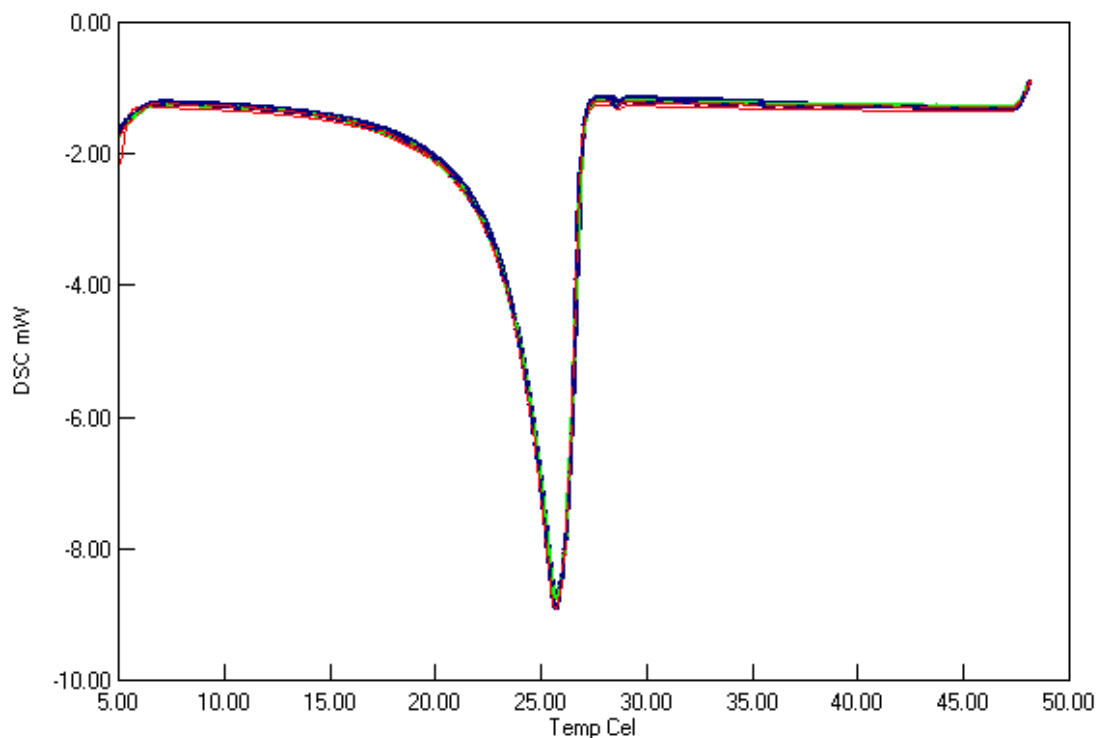


**Figure 5:** DSC test results for MEPCM

**Table 1:** Summary of thermo physical data

Item	Particle size ( $\mu\text{m}$ )	Density ( $\text{kg/m}^3$ )	Porosity (%)	Specific heat ( $\text{J/kg}\cdot\text{K}$ )	Thermal conductivity ( $\text{W/m}\cdot\text{K}$ )	Test No.	Latent Heat ( $\text{kJ/kg}$ )	Melting temperature ( $^{\circ}\text{C}$ )	Energy storage density ( $\text{MJ/m}^3$ )
$\text{Al}_p$	21.5	2700	41%	871	202	-	321[22]	660.4 [23]	-
						1	124	22.3	46.3
MEPCM	15	983	62%	2000	0.09	2	125	22.1	46.7
						3	126	22.2	47.1
						4	124	22.3	46.3
						5	126	22.1	47.1

#### 4.0 SAMPLE DEVELOPMENT

Figs. 6a and 6b show the equipment that were used for producing the composite sample. Fig 6a is a mixing machine type SFM-2, Kejing Group and Fig. 6b is a 100 KN Universal Punching/Testing Machine type SM1000 for punching and recording the dimensional changes in a material thickness with respect to applied compaction pressure. Initially, the mixing machine was prepared by filling the mixing bowl with nitrogen gas in order to prevent any possible dust explosion from the aluminium powder. Quantity of MEPCM (90% by weight) plus 10% by weight of aluminium powder were then mixed together for 30 minutes at a speed of 200 rpm. The final mixture was then emptied into the instrumented single punch press to produce samples of 3g tablets at applied pressures of 2.8, 7.6, 14.8, 29.5, 47.8 and 56.9 MPa with a circular flat-faced die punch. Each tablet was measured at 30mm in diameter and 5~5.3mm in thickness as shown by the sample in Fig. 7.



(a)



(b)

**Figure 6:** Manufacturing equipment



**Figure 7:** Al<sub>p</sub>-PCM tablet sample

## 5.0 RESULTS AND DISCUSSIONS

### 5.1 Porosity

The data collected from the measurements of forces on the punches and the displacement of the upper and lower punches were used in Eq. 17 to calculate the porosity of the samples.

$$\varepsilon(\tau) = 1 - \frac{4m}{\pi h_{\tau} d^2 \rho_p} \quad (17)$$

Where  $m$  is the weight,  $h$  is the thickness,  $d$  is the diameter and  $\rho_p$  is the density of the sample.

Fig. 8 shows the variations in porosity levels with respect to samples produced at different applied pressures. It can be seen that the porosity levels did change after each applied load was removed thus demonstrating the presence of the decompression phenomenon and the extent of plasticity in the samples. On the whole the series of tests revealed a differential porosity level of 20-25% between decompression and compression stages with an average value of 23.8% as against the pre-compaction level of 62%.

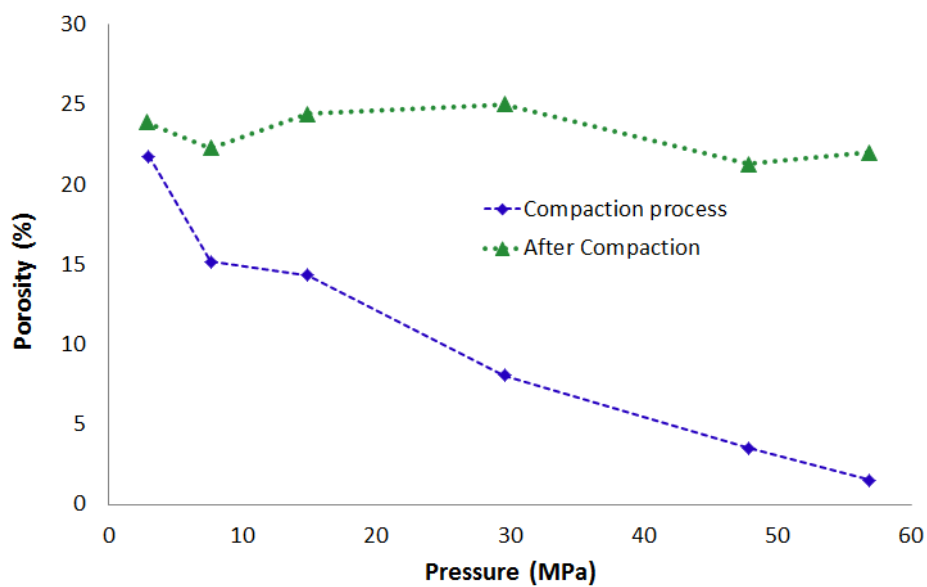


**Figure 8:** Porosity against applied pressure

## 5.2 Latent heat capacity and thermal conductivity

Since the porosity levels in the samples were found to be almost of the same values, it was decided to conduct the latent heat capacity and conductivity tests on any one of them. The type produced with 2.8MPa applied pressure was therefore selected as a representative sample. For the benefit of repeatability, it was tested five times with a DSC equipment. As shown in Fig. 9, the heat flux profiles are similar to each other thus confirming its thermal stability. The sample achieved an average latent heat



value of 111.8 kJ/kg with a melting temperature of 22.2°C. Even though this represents about 10% reduction in the latent heat storage capacity, which is attributed to the presence of the aluminium powder, the mean energy storage density increased by about 97% i.e. from 46.6MJ/m<sup>3</sup> to 91.76MJ/m<sup>3</sup>. The thermal conductivity was also tested over the same number of times with a KD2 Thermal Analyser and obtained a mean value of 2.3 W/m•K at 22.2 °C, which is about 25 times higher than the raw MEPCM. (See the summarised results in Tab. 2). The increase in thermal conductivity also validates the analysis of the profiles of the theoretical models in Fig. 1 where lower porosity values due to compaction resulted in higher conductivities.

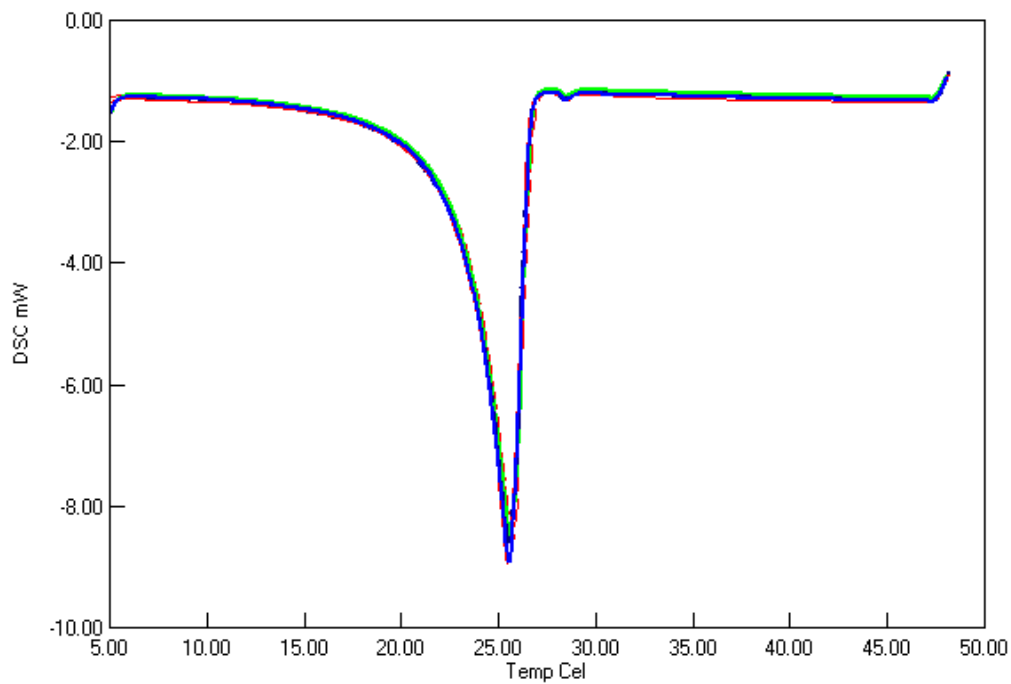


**Figure 9:** DSC test results of Al<sub>p</sub>-PCM tablet

**Table 2:** Summary of mean measured thermophysical data of sample

Item	Packed Density (kg/m <sup>3</sup> )	Porosity (%)	Thermal conductivity (W/m·K) (20-22C)	Latent Heat of (kJ/kg)	Melting temperature (°C)	Energy storage density (MJ/m <sup>3</sup> )
Al <sub>p</sub> -PCM	800	23.8	2.3	111.8	22.2	91.8
MEPCM	373.5	62	0.09	124.8	22.2	46.6

### 5.3 Microscopic structure

A Scanning Electron Microscope (Hitachi S-4800 SEM) was used to examine any structural damage to the tested sample as a result of the applied pressure. Fig. 10 shows the SEM image at pre-compaction stage of the sample and with the aluminium particles fairly dispersed amongst the MEPCM particles. The microscopic image in Fig. 11 shows no sign of any fragmentation of the MEPCM particles after a pressure of 2.8 MPa was applied. However, for the purpose of comparison, the SEM image in Fig. 12 reveals far more damage to the MEPCM particles when a pressure of 29.6 MPa was applied in producing the tablet. It is therefore quite clear that applied pressures have to be controlled and optimised for different particle sizes.

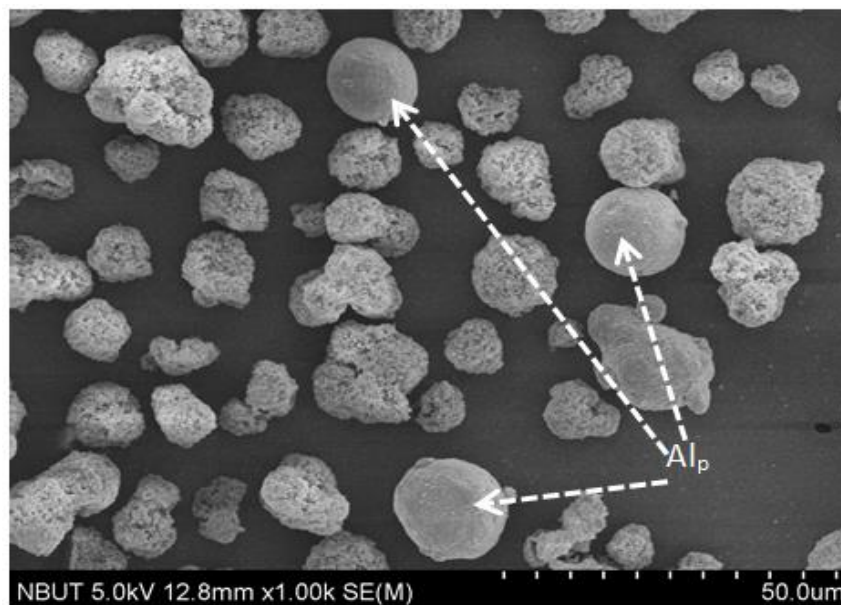


**Figure 10:** SEM image of tablet -before compaction

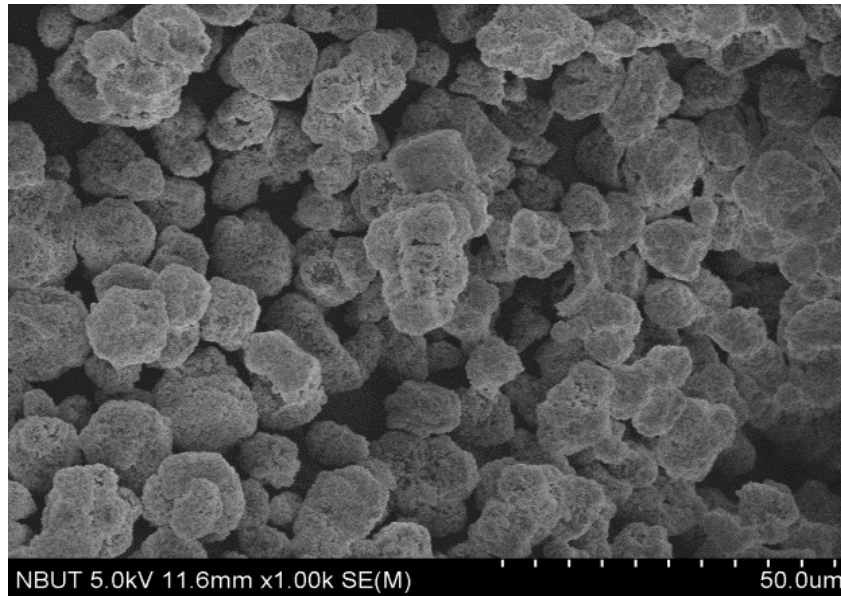


**Figure 11:** SEM image of tablet at 2.8MPa

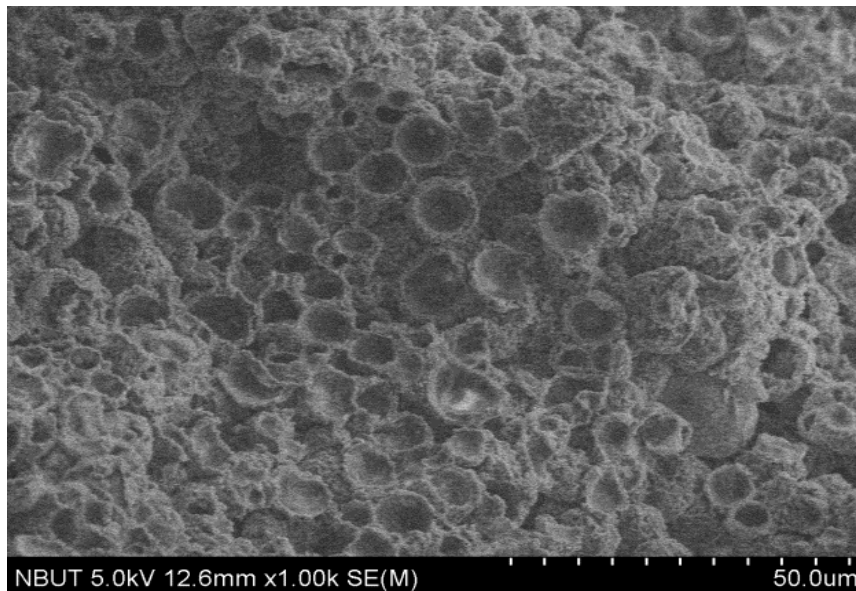


**Figure 12:** SEM image of tablet at 29.6MPa

## 6.0 CONCLUSIONS

The study has demonstrated that the concept of developing a non-deform phase change material possessing high conductivity and high energy storage density could be achieved within certain boundary conditions. The theoretical and experimental investigations have shown that compaction process could reduce porosity level and

increase conductivity and energy storage density of a composite material. Even though the tested sample experienced some measure of plastoelasticity due to decompression, it achieved an average porosity of 23.8% as against the pre-compaction level of 62%. There was also no sign of any fragmentation of the MEPCM particles after a pressure of 2.8 MPa was applied. It was however noticeable in the Fig. 12 that higher pressure could cause structural damage to the MEPCM particles and therefore applied pressures need to be optimised for different particle sizes.

The specific findings may be summarised as follows:

- The mean energy storage density increased by about 97% i.e. from 46.6MJ/m<sup>3</sup> to 91.76MJ/m<sup>3</sup>
- Thermal conductivity increased to 2.3W/m•K which is about 25 times higher than the raw MEPCM

In general, the study has given an insight into a unique method of developing high energy storage composite phase change materials for application in buildings and other sectors. Further work towards minimising the effect of decompression and achieving stronger energy storage tablets at relatively low compaction forces is however encouraged. Another area of further investigation is the likelihood of any negative effect of compaction on the dynamics of material system during operation as a result of volume changes in the PCM particles and any sign of material degradation.

## **ACKNOWLEDGEMENTS**

The authors wish to thank the Ningbo Science and Technology Bureau, China for supporting this research under the Key Laboratory of Integrated Thermal Energy Storage Technologies (ITEST) for buildings project.

## REFERENCES

- [1] Neto, A.H., Fiorelli, F.A.S., “Comparison between detailed model simulation and artificial neural network for forecasting building energy consumption,” *Energy and Buildings*, Vol. 40, 2008, pp. 2169-2176.
- [2] IEA 2011, “Technology Roadmaps - Energy-efficient Buildings: Heating and Cooling Equipment”
- [3] <http://www.environmentalleader.com/2009/04/27/building-sector-needs-to-reduce-energy-use-60-by-2050/>
- [4] Entrop, A.G., Brouwers, H.J.H., Reinders, A.H.M.E., “Experimental research on the use of micro-encapsulated Phase Change Materials to store solar energy in concrete floors and to save energy in Dutch houses,” *Solar Energy*, Vol. 85, Issue 5, 2011, pp. 1007-1020.
- [5] Darkwa, K., O’Callaghan, P.W., “Simulation of phase change drywalls in a passive solar building,” *Applied Thermal Engineering*, Vol. 26, Issue 8-9, 2006, pp. 853-858.
- [6] Darkwa, J., “Mathematical evaluation of a buried phase change concrete cooling system for buildings,” *Applied Energy Journal*, Vol. 86, 2009, pp. 706-711.
- [7] M. Hunger, A.G. Entrop, I. Mandilaras, H.J.H. Brouwers, M. Founti, The behaviour of self-compacting concrete containing-micro-encapsulated phase change materials, *Cement and Concrete Composites*, 31 (2009) 731-743.
- [8] I. Cerón, J. Neila, M. Khayet, Experimental tile with phase change materials (PCM) for building use. *Energy and Buildings*, 43(8) (2011) 1869-1874.
- [9] A. SarI, Form-stable paraffin/high density polyethylene composites as solid-liquid phase change material for thermal energy storage: preparation and thermal properties, *Energy Conversion and Management*, 45(13-14) (2004) 2033-2042.
- [10] J. Li, P. Xue, H. He, W. Ding, J. Han, Preparation and application effects of a novel form-stable phase change material as the thermal storage layer of an electric floor heating system, *Energy and Buildings*, 41(8) (2009) 871-880.
- [11] A.M. Borreguero, M. Luz Sánchez, J.L. Valverde, M. Carmona, J.F. Rodríguez, Thermal testing and numerical simulation of gypsum wallboards

- incorporated with different PCMs content. *Applied Energy*, 88(3) 2011 930-937.
- [12] D. Feldman, D. Banu, D.W. Hawes, Development and application of organic phase change mixtures in thermal storage gypsum wallboard, *Solar Energy Materials and Solar Cells*, 36(2) (1995) 147-157.
- [13] J. Darkwa, T. Zhou, Enhanced laminated composite phase change material for energy storage. *Energy Conversion and Management*, 52(2) (2011) 810-815.
- [14] J. Berggren, G. Frenning, G. Alderborn, Compression behaviour and tablet-forming ability of spray-dried amorphous composite particles. *European Journal of Pharmaceutical Sciences*, 22(2-3) (2004)191-200.
- [15] <http://www.pharmainfo.net/reviews/compaction-pharmaceutical-powders>
- [16] K. Marshall, Compression and consolidation of powdered solids. In: *The Theory and Practice of Industrial Pharmacy*. L. Lachman, H.A. Lieberman, J.L. Kanig, (Eds.) 3<sup>rd</sup> Edition (1986) Lea & Febiger, Philadelphia, 66-99.
- [17] M.J. Bodga, Tablet compression: Machine theory, design and process troubleshooting (2002). In: *Encyclopedia of Pharmaceutical Technology*. Swarbrick J and Boylan J (Eds). Marcel and Dekker Inc., USA, Vol. 3: 2669 – 2688.
- [18] R.W. Heckel, Density-pressure relationships in powder compaction. *Trans. Metall. Soc. AIME*, 221(1961) 671-675.
- [19] S.T. David, L.L. Augsburger, Plastic flow during compression of directly compressible fillers and its effect on tablet strength, *J. Pharm. Sci.*, 66 (1977) 155-159.
- [20] M. Kohout, A.P. Collier, F. Stepánek, Effective thermal conductivity of wet particle assemblies, *International Journal of Heat and Mass Transfer*, 47(25) (2004) 5565-5574.
- [21] F. Fichtner, A. Rasmuson, G. Alderborn, Particle size distribution and evolution in tablet structure during and after compaction, *International Journal of Pharmaceutics*, 292 (2005) 211–225
- [22] [http://www.engineeringtoolbox.com/latent-heat-melting-solids-d\\_96.html](http://www.engineeringtoolbox.com/latent-heat-melting-solids-d_96.html)
- [23] [http://www.engineeringtoolbox.com/melting-temperature-metals-d\\_860.html](http://www.engineeringtoolbox.com/melting-temperature-metals-d_860.html)